Balloon Observations of X Rays in the Auroral Zone

3. High Time Resolution Studies

K. A. ANDERSON AND D. W. MILTON

Department of Physics and Space Science Laboratory
University of California, Berkeley

Abstract. During three separate balloon flights made in the auroral zone, it was found that the precipitation of energetic electrons occurred by means of short, impulsive bursts having definite features. Since these bursts were found to have no substructure, they have been called microbursts. They are homogeneous with respect to rise time and duration; the decay time is less consistent. Periodic studies of microburst spacings have revealed no strong period, but a departure from purely random behavior can be shown. Some of the characteristic times of microbursts can be explained on the basis of electron motions on the auroral zone line of force.

INTRODUCTION

One of the most remarkable and long recognized features of the auroral zone X-ray fluxes [*Anderson,* 1964] is the large fluctuations that occur in their intensity from hour to hour, minute to minute, and in much shorter time intervals. Figure 1 is an example of a highly structured event showing spacings between X-ray peaks down to times as short as five seconds, the limit imposed by the instrumentation in that case. The first attempt to treat fluctuations of X-ray intensity in a systematic way was that of *Winckler et al.* [1962]. These workers applied a power spectrum analysis to about one hour's X-ray data taken at Minneapolis during the world-wide magnetic storm of September 30 through October 1, 1961. A power spectrum analysis was also used on X-ray data taken during a recurrent geomagnetic storm on September 25, 1961, at Flin Flon, Canada, an auroral zone site. Though peaks appeared in the power spectrum of the Minneapolis data, thus revealing significant periodicities, the power spectrum of the auroral zone data showed no peaks. No other studies to date have provided evidence for periodic behavior of auroral zone X-ray fluxes despite substantial observational efforts. It is therefore quite clear that periodic phenomena by no means play a dominant role in the precipitation of electrons in the auroral zone. The observational studies to be reported here represent an attempt to further explore the possible existence of periodic effects in auroral zone electron precipitation. Equally important, by means of large area detectors and fast response electronic circuitry, the temporal structure of X-ray bursts has been examined over the region of time intervals from about ten seconds down to a few milliseconds.

DESCRIPTION OF INSTRUMENTATION

The main objective of the experiment to be discussed here is to examine temporal features in the auroral zone X-ray fluxes above 30-kev photon energy with resolution to intervals as short as a few milliseconds. Further, we want to apply high resolution analysis to small and moderate auroral X-ray fluxes which occur with much greater frequency than do extremely high fluxes, thus obtaining a much more representative study of auroral zone processes involving energetic electrons. To accomplish this objective, the detector must be very large in order to effectively produce statistically significant samples within such short times, and the electronic circuitry, including the telemetry link, must be able to faithfully respond to these rapid changes.

Since the apparatus employed in this experiment is markedly different from that used in past studies of auroral zone X rays, it will be described in some detail. A block diagram of the flight apparatus is given in Figure 2. The X-ray detector is a thallium-activated sodium iodide scintillation crystal five inches in diameter and one-half inch thick. The area of this crystal weighted isotropically with respect to solid angle

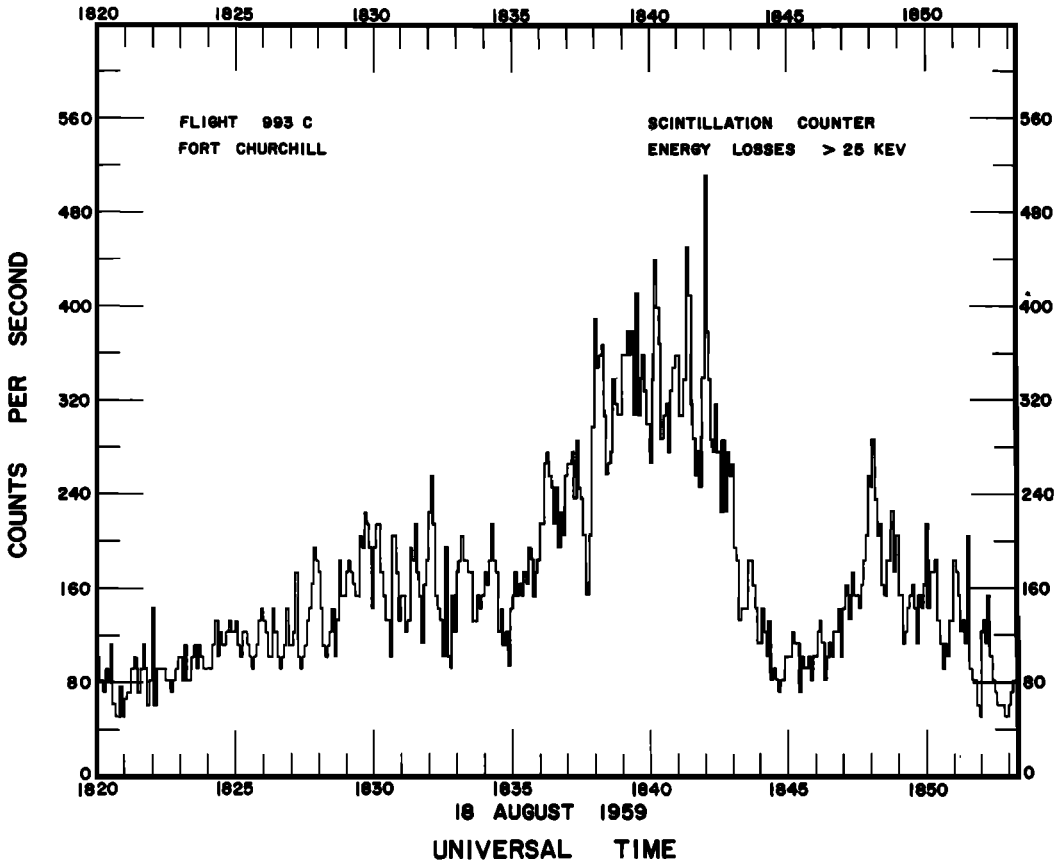

Fig. 1. This highly structured event occurred over an $L = 8$ auroral zone site in 1959. The sharp spikes may be microburst trains with individual microbursts unresolved.

over the upper hemisphere is 76 cm^2. The entrance window for the X-ray flux is 0.14 g cm^{-2} of aluminum. The transmission through this window weighted for an isotropic X-ray flux is 80% at 30 kev, 90% at 40 kev, and 99% at 80 kev. The lower hemisphere of the crystal is shielded by about 3 g cm^{-2} of glass and 1 g cm^{-2} of aluminum. Since the atmosphere can Compton scatter X rays quite efficiently, an upward moving X-ray flux must be expected. The transmission for an isotropic upward moving X-ray flux is 4%, 10%, and 80% at the above energies. Thus a scattered contribution from the lower hemisphere will appear at the detector and will be most important at the highest photon energies. The energy resolution of the detector is limited by two factors. The inherent resolution due to photoelectron statistics is about 15% FWHM. Nonuniform photoelectron collection in the photomultipliers contributes typically about a 20% energy spread in the tubes used. The over-all energy resolution was determined for each of the detectors flown by uniformly irradiating the detector with a 60-kev X-ray source. The over-all energy resolution due to detector effects found in this way varied from 25% to 35% FWHM (full width at half maximum).

The output pulses of the photomultiplier are sorted by a discriminator into three energy groups. The 30- to 60-kev window and the 60-kev integral rates are passed to electronic circuits which convert the counting rates to analog voltage levels in a manner to be discussed more fully below. The 30-kev integral rate is fed to binary scalers having a scaling factor of 8192. The main purpose of the digital channel is to verify proper performance of the analog channels. Energy calibrations were made on each flight unit by means of several radioactive

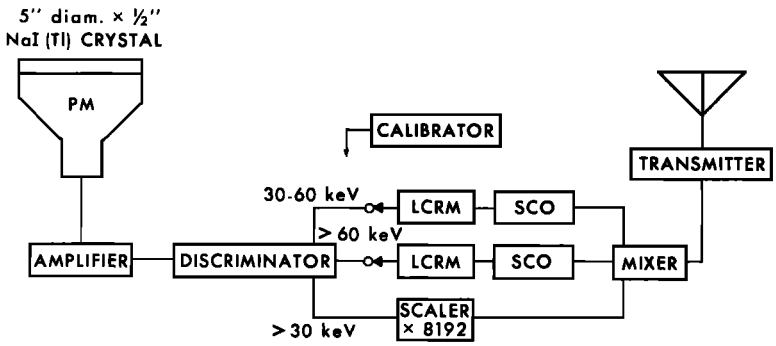

Fig. 2. Block diagram of the apparatus used in the high time resolution studies. It is characterized by a very large detector and by the fact that nearly all the information generated by the detector is passed by the electronic circuits to the ground station. This apparatus has been flown successfully on thirteen flights during a two-year period.

sources. A final calibration was made just before each flight; we believe the error in energy determination to be about ±10%. The average photon energy detected in the two energy regions investigated can be obtained by averaging a typical auroral zone X-ray spectrum over these intervals. Using a differential spectrum reported by *Anderson and Enemark* [1960], which varied as $(h\nu)^{-s}$, the weighted average for the window is 40 kev, and for the 60-kev integral edge the average energy is 80 kev. As has been mentioned, the energy resolution in these detectors is typically 30% FWHM. The average energies in the analog channels are thus 40 ± 6 kev and 80 ± 12 kev, where the deviations indicate the half-intensity points in the distributions, which are nearly Gaussian.

We next describe the operation of the circuits in the two analog channels. Whenever an energy loss in the scintillation crystal was of proper size to trigger the discriminator circuit, this circuit caused the generation of a 3.5-μsec pulse carrying a fixed amount of charge. These charges were fed to a parallel combination of a smoothing capacitor and a network of resistors and diodes. An increase in counting rate thus caused the fixed charges to be fed into this combination more frequently and the output voltage to rise. At the same time, however, the increased voltage caused the parallel resistance to be reduced owing to biasing action on the diodes. The parameters were chosen to give a nearly logarithmic relation between the counting rate and the voltage output. This circuit is therefore a logarithmic count rate meter (LCRM), and we refer to its output as the analog counting rate.

The advantage of the LCRM technique over binary scaled data is that the entire information content of signals from the detector is retained at all counting rates. Binary scalers always process the data before telemetry or storage, and hence effectively lose information in a preset format of the scaling factor or factors. The LCRM passes nearly all detector information through the telemetry link to the laboratory, where flexible and powerful information handling techniques can be applied.

An additional advantage of the LCRM method is that with the data in analog form a wide range of data handling techniques is available for analysis. Among these is electrical filtering. By means of filters it is easily possible to automatically reject fluctuations which are not statistically significant and to pass only those that are. This method can be readily and conclusively checked in any data reduction procedure by applying random signals, most conveniently those from radioactive sources. This procedure, in effect a statistical error analysis, is carried out continuously, whereas in digital techniques only spot checks are ordinarily feasible.

The response time of the analog counting rate is about three milliseconds when a counting rate of a few thousand counts per second is suddenly applied to the input. Figure 3*a* shows this feature and the decay characteristics of the LCRM. The fast response times of the LCRM make the individual counts discernible at low

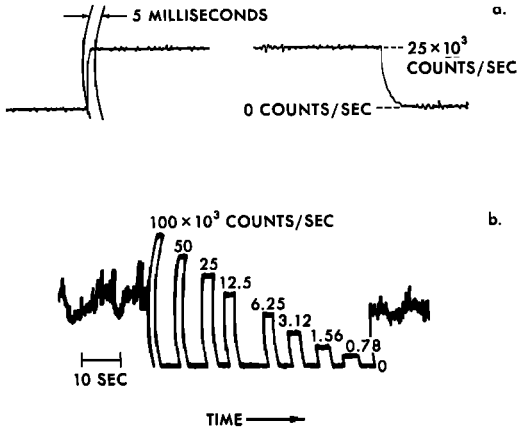

Fig. 3. The fast rise and decay characteristics of the logarithmic counting rate circuits. Also shown is one of the in-flight calibration sequences. These were made every fifteen minutes.

rates, as can be seen in Figure 4*a*. Because the LCRM has a dynamic range of 1000:1, it is suited for the study of the highly variable auroral zone X-ray intensities.

In addition to camparing analog data with scaled data, we used a variety of methods to check the LCRM circuits during flight. At fifteen-minute intervals during the flights, a commutator disconnected the photomultiplier output and injected into both LCRM circuits nine known stable counting rates generated by an oscillator in a sequence ranging from zero to 100,000 cps. Figure 3*b* shows the analog counting rate during a calibration sequence. Not only is the counting rate calibration checked inflight in this manner, but the time constants of the LCRM circuits are also obtained throughout the flight. During the time when the commutator applies zero counting rate to each LCRM, the total system noise can be observed. Errors from this source are less than 10% in all counting rate determinations. Another routine check on the operation of all LCRM circuits was the comparison of the cosmic ray background level during the flights with the response of a flight quality unit kept in the laboratory to a radioactive source. Since both of these are sources of random counts, the responses must be the same when the LCRM circuitry is operating properly as shown in Figure 4*b* and 4*c*. To confirm that the apparatus was working within acceptable temperature limits, the temperature of the circuits was telemetered. Printed circuit construction and uniform testing procedures insured that the flight instruments were essentially identical. The analog counting rates were telemetered over a minimal noise FM/FM system with subcarrier frequencies above 10,000 cps to avoid impairment of the fast LCRM response times. At the receiving station the subcarrier frequencies containing the analog counting rates were put on magnetic tape by high quality tape recorders. A crystal controlled tape speed reference signal was applied to the data tapes at the ground station simultaneously with the data to insure that power line frequency variations or tape recorder speed variations could not affect the data. This signal was continuously recorded on a second channel of the tape recorder, and in the data reduction procedures it was handled in the same manner as the data signal. After discrimination the signal from the crystal controlled oscillator was electrically subtracted from the analog data voltage level. This procedure gives an analog counting rate voltage fully compensated for spurious

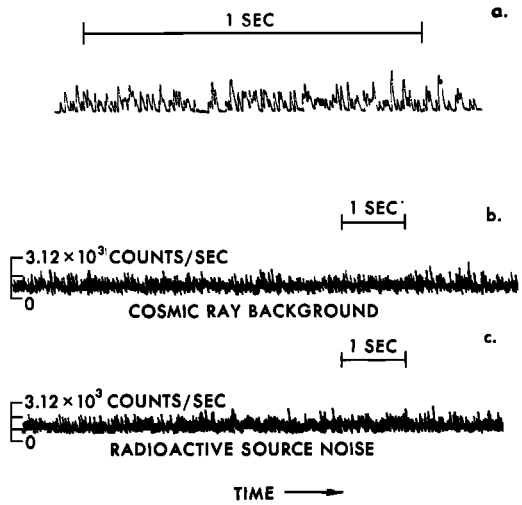

Fig. 4. (*a*) The response of the apparatus to single counts, which are the smallest of the spikes seen. The stretch of data shown was taken during a balloon ascent at 10,000 feet altitude where the cosmic ray background count was still quite low. (*b*) and (*c*) The response of the count rate circuits to the high cosmic ray background rate at 110,000 feet altitude and to a radioactive source producing the same counting rate. As would be expected, since both are from random event generators, their appearance is the same.

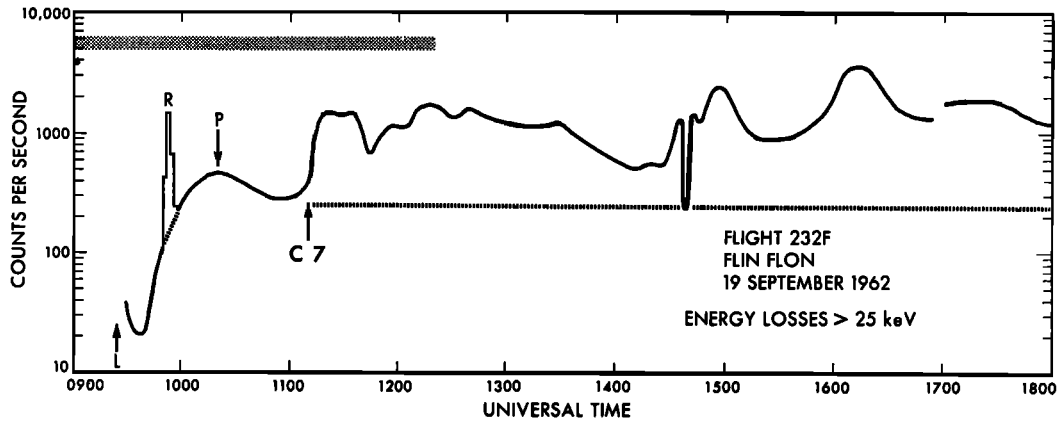
10,000
1000
100
10
COUNTS PER SECOND
R
P
C 7
L
FLIGHT 232F
FLIN FLON
19 SEPTEMBER 1962
ENERGY LOSSES > 25 keV
0900
1000
1100
1200
1300
1400
1500
1600
1700
1800
UNIVERSAL TIME

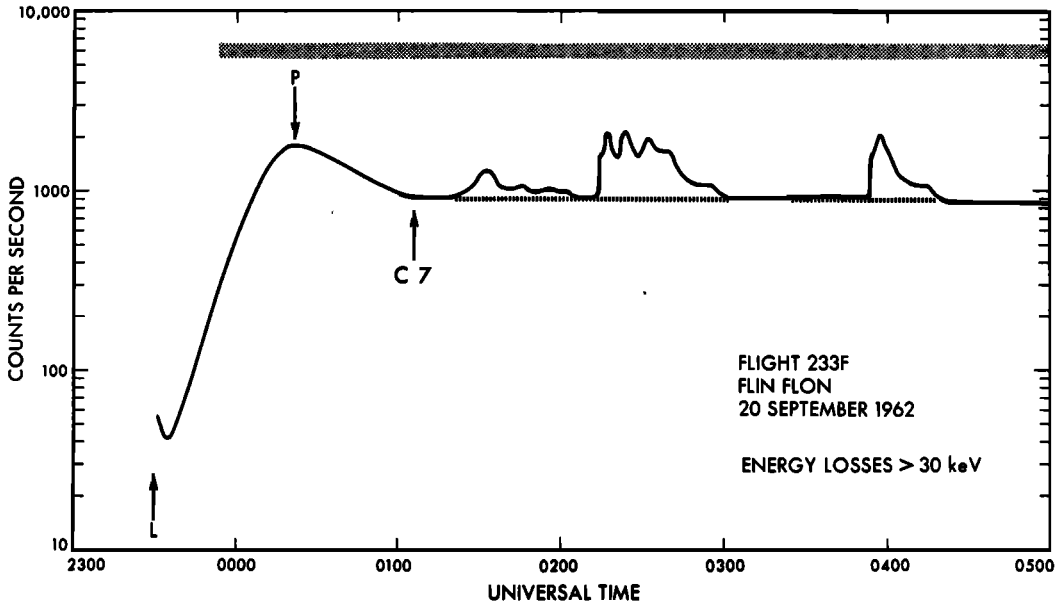
10,000
1000
100
10
COUNTS PER SECOND
P
C 7
L
FLIGHT 233F
FLIN FLON
20 SEPTEMBER 1962
ENERGY LOSSES > 30 keV
2300
0000
0100
0200
0300
0400
0500
UNIVERSAL TIME

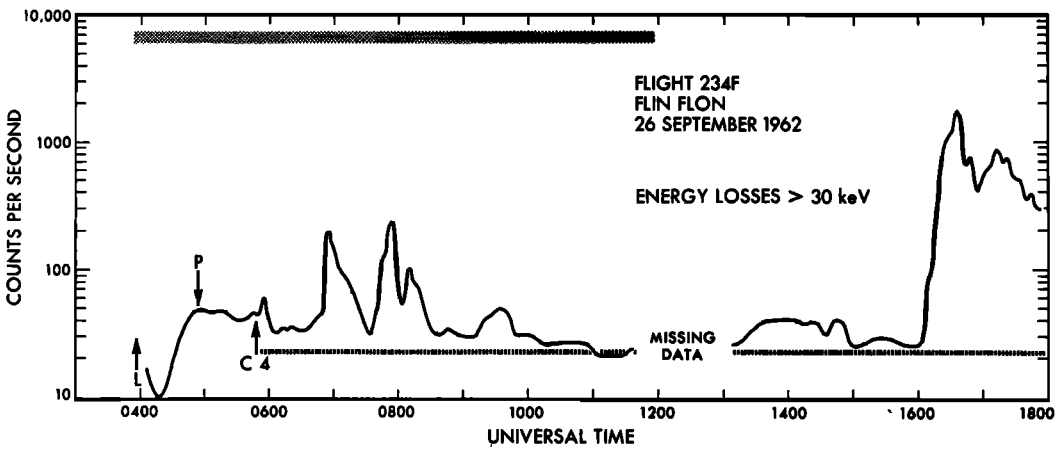
10,000
1000
100
10
COUNTS PER SECOND
FLIGHT 234F
FLIN FLON
26 SEPTEMBER 1962
ENERGY LOSSES > 30 keV
P
C 4
L
MISSING
DATA
0400
0600
0800
1000
1200
1400
1600
1800
UNIVERSAL TIME

Fig. 5*a*

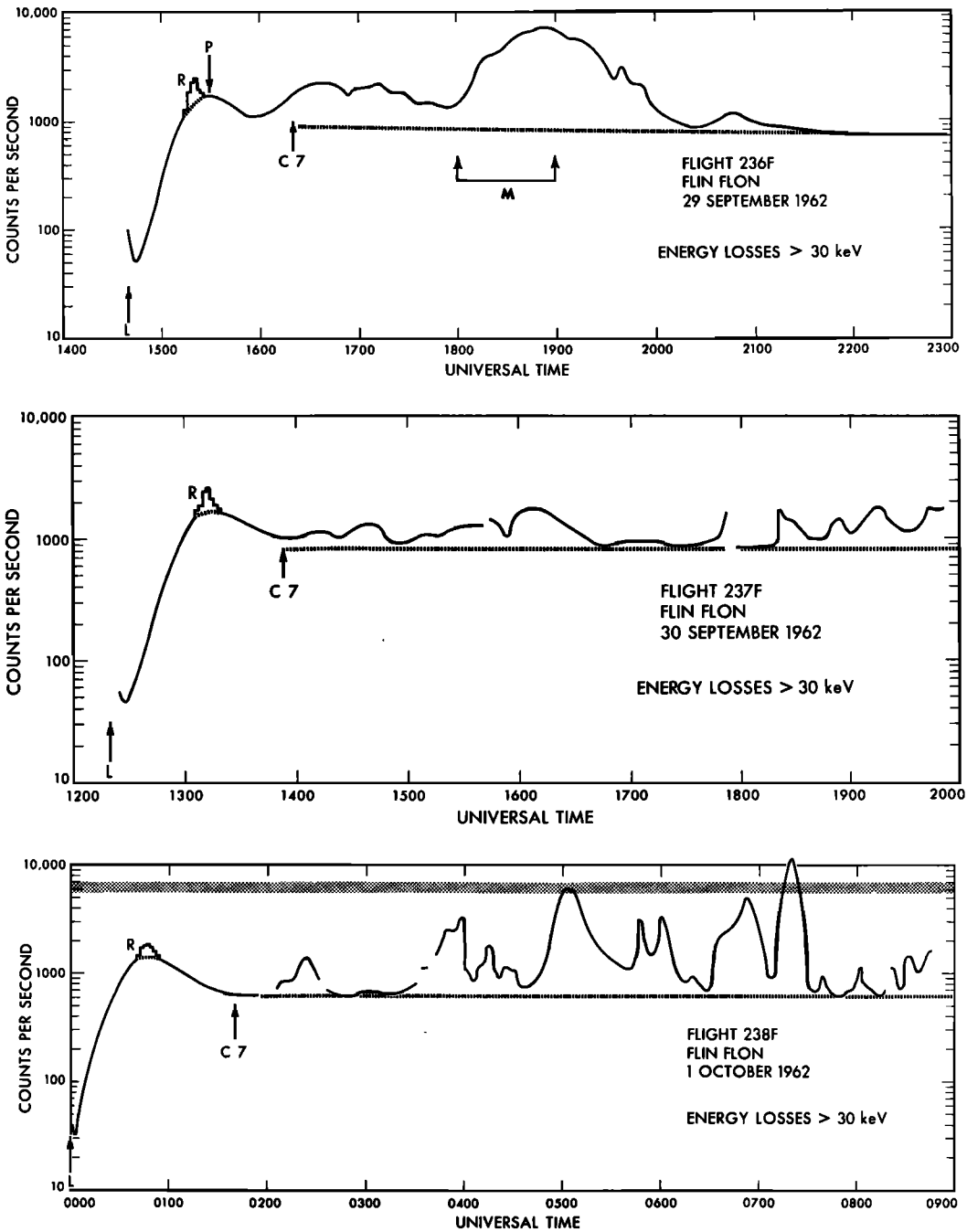
10,000
1000
100
10
COUNTS PER SECOND
P
R
C 7
M
L
FLIGHT 236F
FLIN FLON
29 SEPTEMBER 1962
ENERGY LOSSES > 30 keV
1400
1500
1600
1700
1800
1900
2000
2100
2200
2300
UNIVERSAL TIME
10,000
1000
100
10
COUNTS PER SECOND
R
C 7
L
FLIGHT 237F
FLIN FLON
30 SEPTEMBER 1962
ENERGY LOSSES > 30 keV
1200
1300
1400
1500
1600
1700
1800
1900
2000
UNIVERSAL TIME
10,000
1000
100
10
COUNTS PER SECOND
R
C 7
L
FLIGHT 238F
FLIN FLON
1 OCTOBER 1962
ENERGY LOSSES > 30 keV
0000
0100
0200
0300
0400
0500
0600
0700
0800
0900
UNIVERSAL TIME

Fig. 5*b*

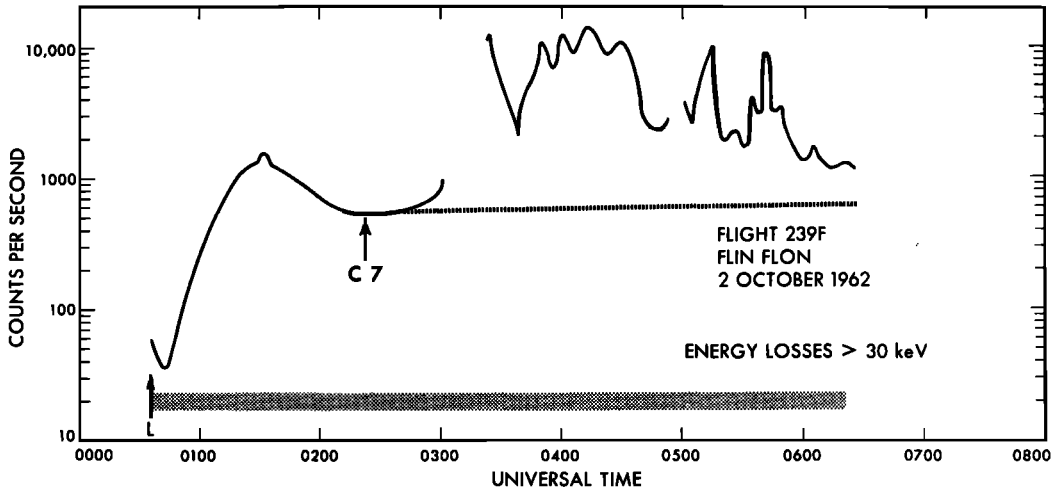

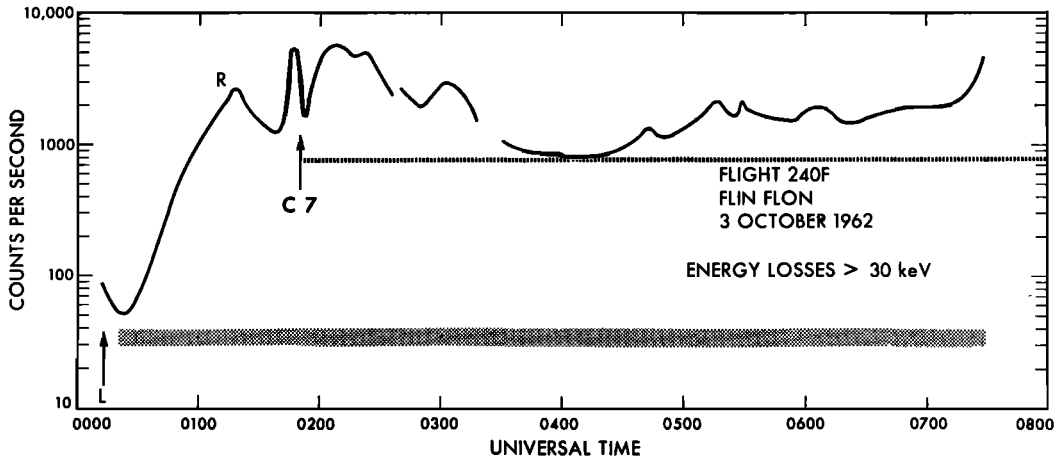

Fig. 5c

Fig. 5. Summaries of the 1962 flights at Flin Flon, Canada. The symbols are: *P*, Pfotzer maximum; *R*, artificial radioactive debris layer; and *C*, time when the balloon reached ceiling altitude. The number following *C* indicates the atmospheric depth at ceiling altitude in g cm^{-2}. *M* indicates the occurrence of microbursts. Calibration sequences produce the open spaces in the data record.

variations due to tape speed fluctuations. The effectiveness of the compensation can be judged at any time by putting a drag on the tape reels as data are being played into the electronic data reduction equipment.

Description of Balloon Flights

Eight instruments were flown in 1962 and seven in 1963 from Flin Flon, Manitoba, Canada. This auroral zone site is at 56°N geographic latitude and 102°W longitude. The geomagnetic latitude is 64.5°, corresponding to an *L* value of about 6. The instruments were carried on balloons of 800,000-cubic foot volume to an altitude of 110,000 feet, or an atmospheric depth of 7 g cm^{-2}, which was quite closely maintained throughout the flights. The flights were from 6 hours to about 15 hours in duration, some covering daylight hours and others nighttime periods. The balloons drifted east-southeast from Flin Flon, and were usually a distance of 250 miles away at the termination of the flights.

Figures 5 and 6 show the complete flight records for both series of balloon launches. The

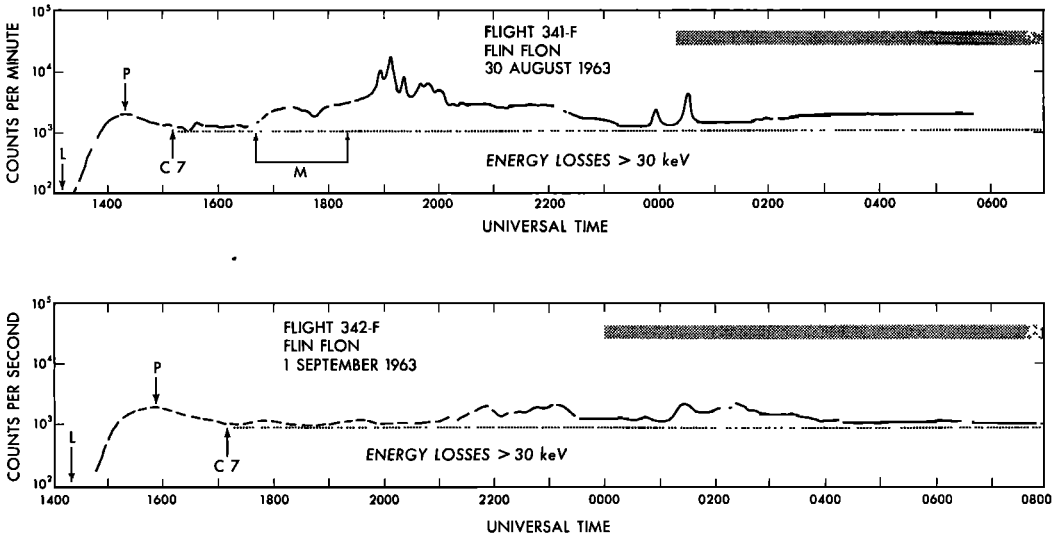

Fig. 6*a*

counting rates plotted there are obtained from the binary scaled output, and temporal features on time scales of one minute and longer will appear. Good quality analog counting rates were obtained for 70 hours from balloons at ceiling altitude in 1962 and 90 hours in 1963.

Methods of Data Analysis

The analog counting rate was presented for analysis in two ways. First, by the use of magnetic tape time base changes and appropriate filters, strip chart graphs were made with time scales from 1 cm per 5 msec to 1 cm per 40 sec of real time. Both time calibrations and LCRM calibrations were an integral part of these data records. These strip chart recordings were used for many kinds of visual studies of the analog counting rate and will be described in later sections. Second, using a voltage to frequency converter and electronic counter-printer, the analog counting rate was digitally sampled for 1.25 msec at time intervals of 25 msec after filtering which effectively averaged the analog counting rate over 25-msec periods. These sampled rates

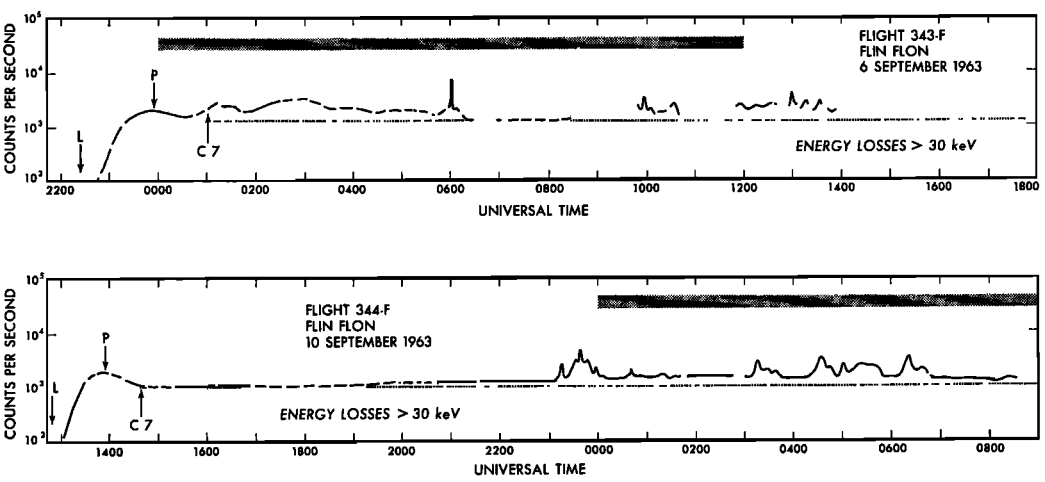

Fig. 6*b*

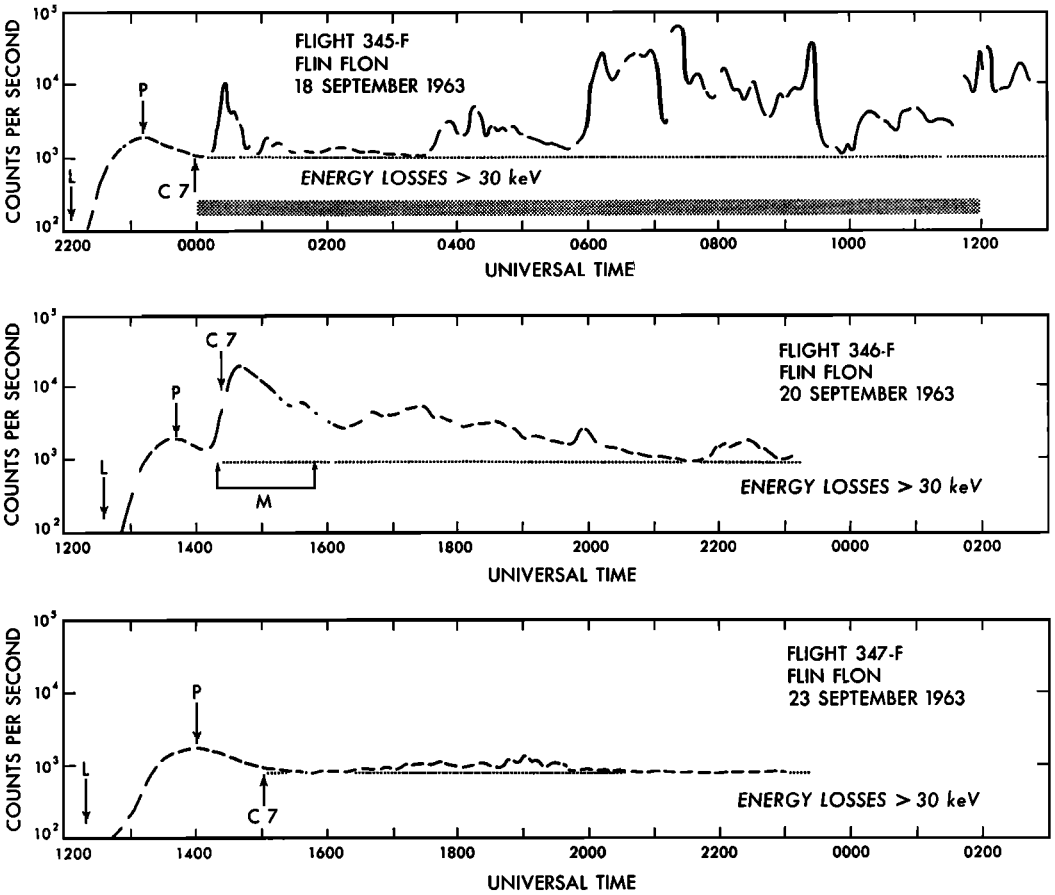

Fig. 6c

Fig. 6. Summaries of the 1963 flights also at Flin Flon. The symbols are the same as for Figure 5.

were put on punched cards and several statistical analyses were carried out on an IBM 7090 computer.

Results

Some properties of microbursts. Approximately 160 hours of high altitude balloon data were obtained in 1962 and 1963 at Flin Flon by the LCRM apparatus. Detectable auroral zone X-ray fluxes were present 100 of these hours. Statistically significant data samples can be obtained at 10-msec resolution with counting rates of about 10^4 sec^{-1}. As can be seen from Figures 5 and 6, rates in excess of this are frequently encountered. These hours of high counting rate data were systematically investigated by visual inspection of strip chart recordings of the analog counting rate. Most of the data were characterized by featureless and slow changes of intensity in time intervals from 10 to 0.01 sec. Figure 7 gives typical examples of the X-ray fluxes at these times. The analysis here will not be concerned with this rather featureless variety of electron precipitation.

Large X-ray detectors and the LCRM together make it possible to observe time structure in the auroral zone X-ray flux on any time scale from a compressed one showing a whole flight to an expanded one showing the influx of small groups of photons. Figure 8*b* shows an expansion of the underscored part of Figure 8*a*. A great deal of time structure in the X-ray fluxes is now visible. As a comparison, purely statistical analog counting rate variations from

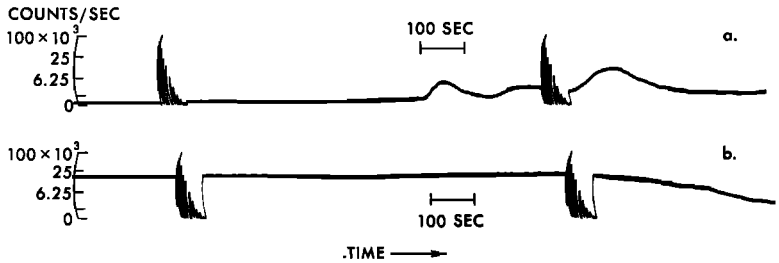

Fig. 7. Examples of auroral zone electron precipitation characterized by slow changes in intensity. The staircase signals are in-flight counting rate calibrations.

a radioactive source produce features which in no way resemble that record. The two interruptions seen in Figure 8*b* are calibration sequences. The filter used to present the analog counting rate graphically has caused the calibration signals to lose some detail.

The next time expansion in Figure 8*c* shows an entirely new set of time structures. The most striking feature is the appearance of bursts of about 0.25-sec duration rising out of a rather uniform auroral zone X-ray background. As we will demonstrate, these bursts have been seen

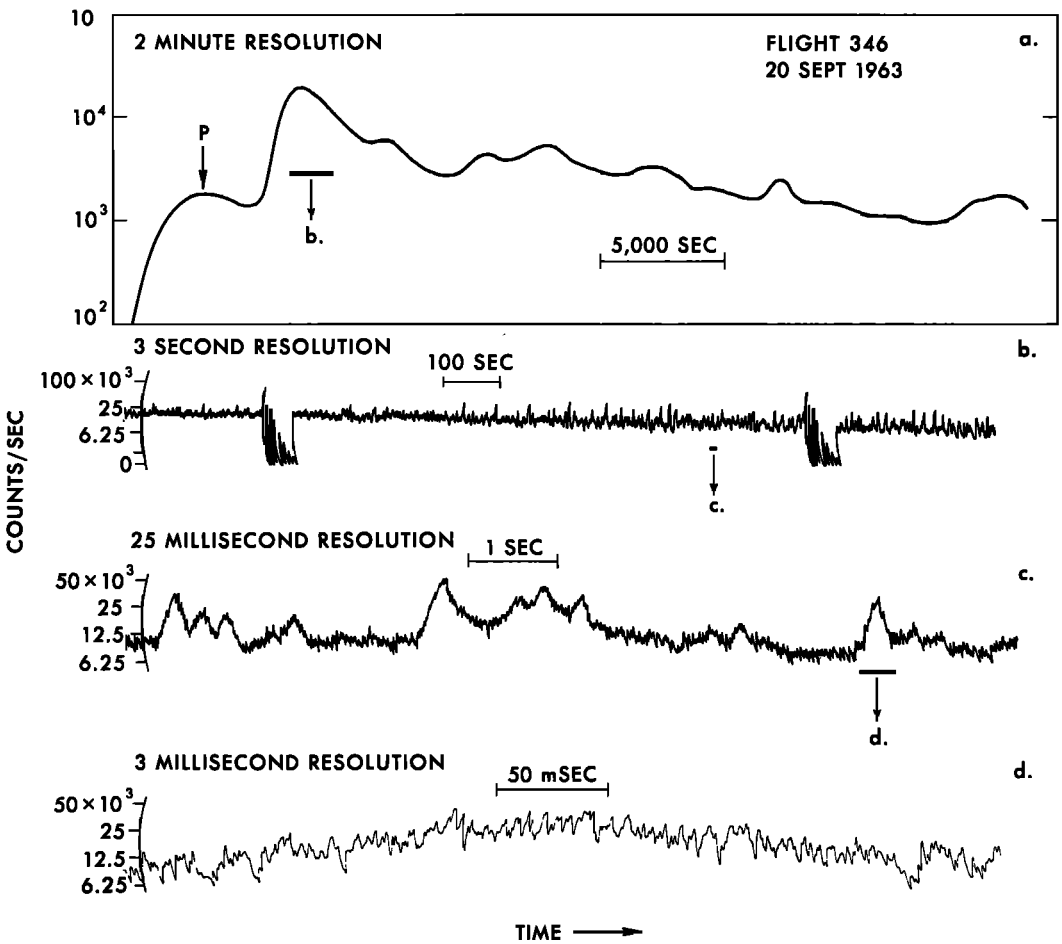

Fig. 8. Successive expansion of a section of data containing microbursts. Part *d* of the figure shows that the microburst contains no further structure. The notches are due to statistical variations.

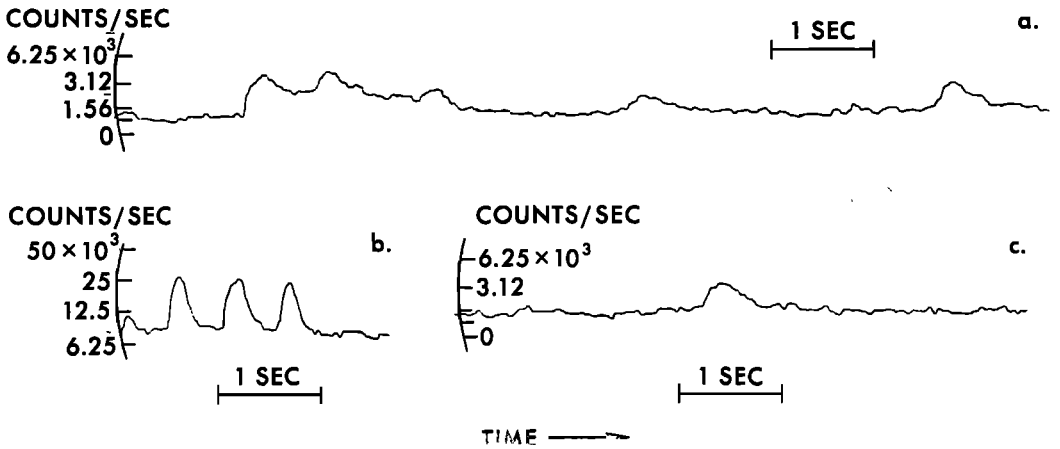

Fig. 9. Examples of microbursts. These have been filtered to remove statistical variations. The structures are seen to occur singly (*c*) or in groups of three or four (*b* and *a*).

on several occasions, and they are a characteristic feature of the auroral zone electron precipitation. Because this entity has quite clearly definable features, we refer to it as a microburst. The spikes seen in Figure 8*b* thus do not have a simple structure but are made up of groups of microbursts.

A further expansion of the time scale in Figure 8*d* shows the important result that the microburst is not an average of still smaller bursts which rise out of the background. The fluctuations which appear in Figure 8*d* are statistical fluctuations in the analog counting rate and have the same appearance when the analog counting rate due to a radioactive source of the same average flux is examined. With high counting rate data, further time expansions beyond that shown in Figure 8*d* so far have not revealed temporal features of interest, although the LCRM and telemetry system are capable of resolution of a few milliseconds.

Microbursts have been encountered to date on three separate balloon flights carrying large crystals and LCRM circuitry. One occurred in 1962 and two in 1963. (*Note added in proof:* A balloon flight on September 8, 1964, again encountered microbursts.) Some immediately apparent features of the microbursts are the following:

1. They occurred for an interval of about 1.5 hours on each occasion. These times are shown in the flight records of Figures 5 and 6. When the microbursts first appeared they were infrequent, then increased in frequency, reaching typically an average of 1 per sec. They finally disappeared by becoming weak in intensity and fading into the background.

2. The microbursts were encountered during daylight hours, mostly before local noon.

3. The microbursts occurred singly but more frequently as double bursts and most often in trains of three or more. Examples are shown in Figures 8*c*, 9, and 10.

4. Regardless of the pattern in which the microbursts occurred, they maintained a definite identity in the sense that the characteristic features of the individual microbursts were not altered by their appearance in groups.

5. The most characteristic and regular feature of the microburst is its duration in time. The width of the bursts at their half intensity points was about 0.25 sec.

6. Although the main feature of the electron precipitation during these times was the presence of microbursts, these were usually superposed on a smooth background of X-ray flux which persisted for as long as several hours.

7. In all cases, however, the presence of microbursts was responsible for significantly enhancing the counting rate when averaged over at least several seconds. Microbursts above a certain size in peak X-ray flux were selected, and their number in each two-minute interval was plotted in Figure 11*a*. The average X-ray flux above 30 kev which was measured by the scalers was plotted for the same two-minute intervals in Figure 11*b*. It can be seen that there

is a definite covariance between the two graphs. In the case selected (August 30, 1963) the microbursts rose directly out of a uniform cosmic ray background and were not superposed on a steady auroral zone X-ray background. The microbursts themselves were thus responsible for producing a significant X-ray flux averaged over times long compared to the characteristic microburst width. Some data from September 20, 1963, shown in Figure 8*c*, exemplify the superposition of microbursts on a rather high auroral zone X-ray background. Even in this case the microbursts contributed substantially to averaged counting rates.

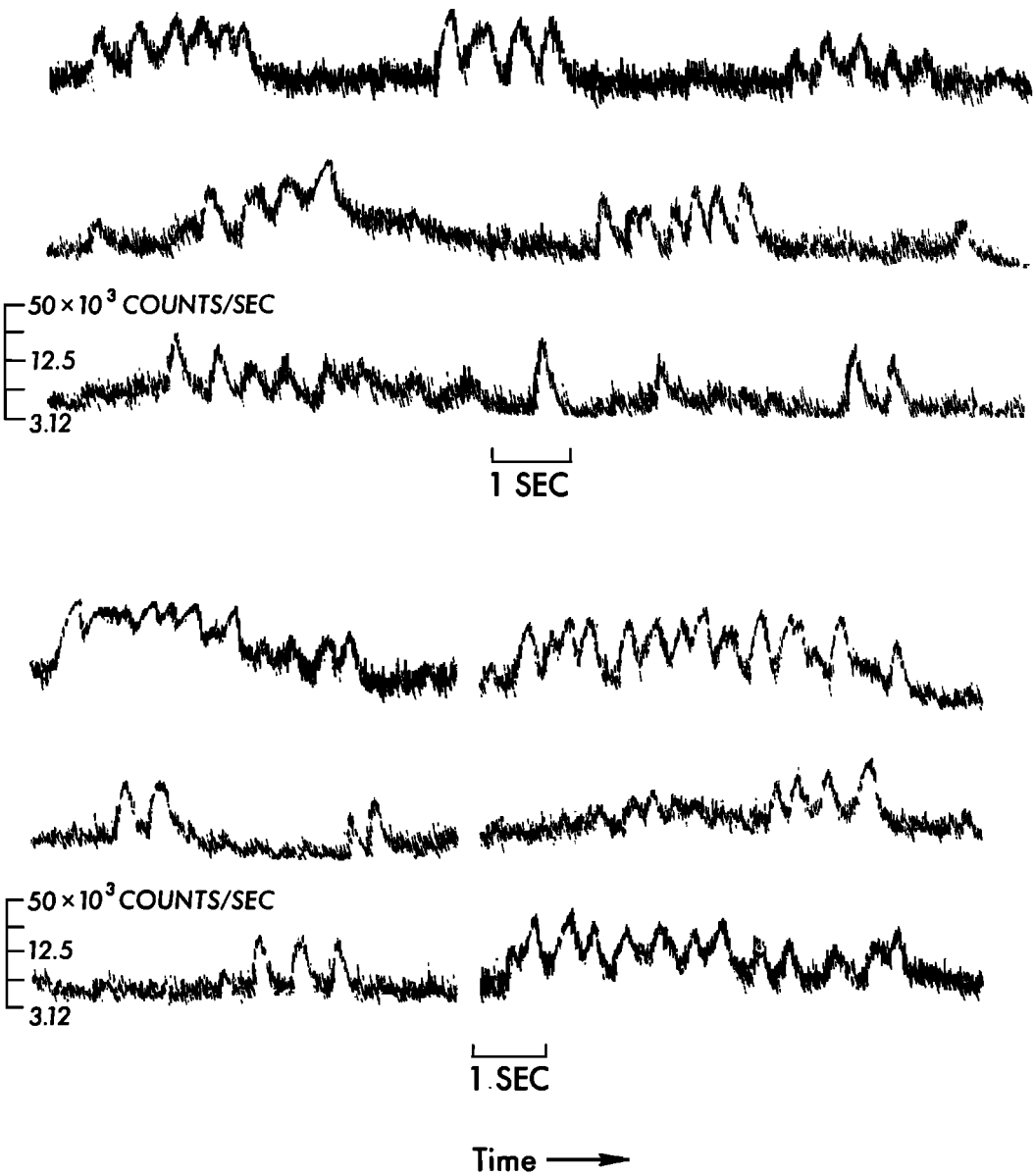

Fig. 10. Further examples of microbursts, showing their occurrence in trains of as many as fifteen individuals. The characteristic but random spacing of the trains is illustrated. This spacing is typically 10 sec. The trains ranged from being completely notched to highly webbed.

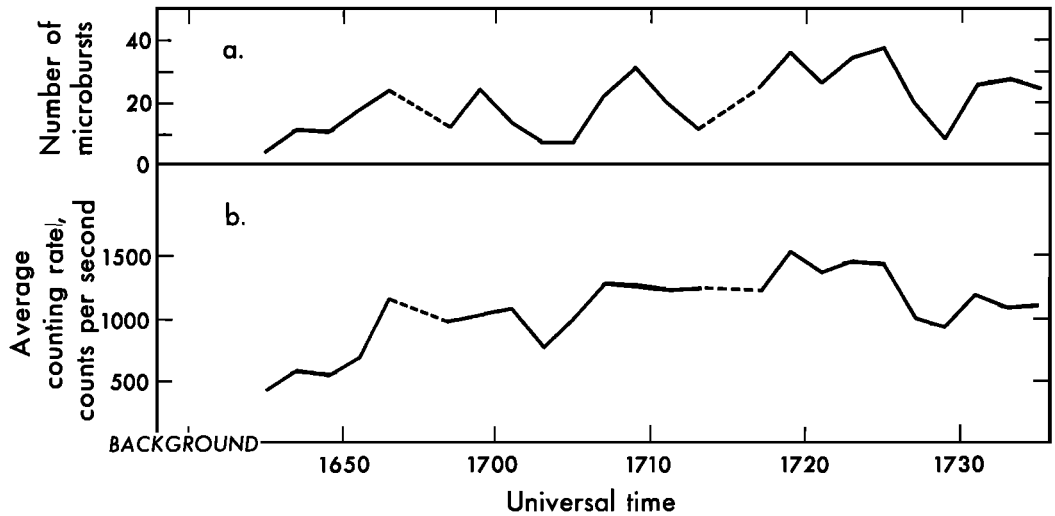

Fig. 11. (*a*) The frequency of microbursts as a function of time during one of the balloon flights. The units are the number of microbursts in a two-minute interval. (*b*) The gross counting rate averaged over many microbursts closely follows the microburst frequency.

8. Several thousand microbursts have appeared on our records and more than 1600 have been subjected to analyses to be described in the rest of this article.

Microburst time profiles. Visual inspection of many hundred microbursts on strip chart recordings gave the impression that they were homogeneous with respect to important time constants such as rise time, duration, and decay time. It was also true that noticeable differences did appear between individual microbursts. In particular, those on one balloon flight had a consistent tendency to be somewhat different from those on another. To investigate objectively these qualitative impressions, composite studies have been made by superposing many individual microbursts. The analog counting rates of the microbursts to be studied were digitized in the manner discussed in the section on Data Analysis Methods. Each digitized microburst contained about thirty points. The microburst peaks were marked, and the digitized analog counting rates were averaged in a way similar to a Chree analysis. The quantity used in the analysis was the logarithm of the scintillation counter rate. Therefore, addition of these digitized analog counting rates and conversion to a linear quantity resulted in the geometric mean of the actual scintillation counter rates.

The composites of 150 microbursts from the August 30, 1963, flight and 60 from the September 20, 1963, flight are shown in Figures 12*a* and *b*, respectively. The August 30, 1963, composite has a duration of about 270 msec measured at the half intensity points. It is seen to have a longer decay time than rise time. The X-ray flux at the peak is about 40 cm^{-2} sec^{-1} above all backgrounds. The high counting rate pedestal on which this composite rises is due to the method of analysis. These microbursts rise out of the cosmic ray background, but the average of smaller microbursts preceding and following the main selected peaks forms the apparent background noticed in that figure. The composite obtained on September 20, 1963, is essentially symmetrical in shape and has a narrower width of 160 msec. The large counting rate on which it is situated is mainly due to a large, slowly varying auroral zone X-ray background at these times. The peak X-ray flux above all backgrounds for this composite is 140 cm^{-2} sec^{-1} between 30 and 60 kev. Most of the individual microbursts forming this composite were preceded and followed by equally large microbursts. This accounts for the increase before and after the main peak seen in Figure 12*b*.

We see that the rise time and main peak duration of the two statistical averages based on different balloon flights are similar. The decay

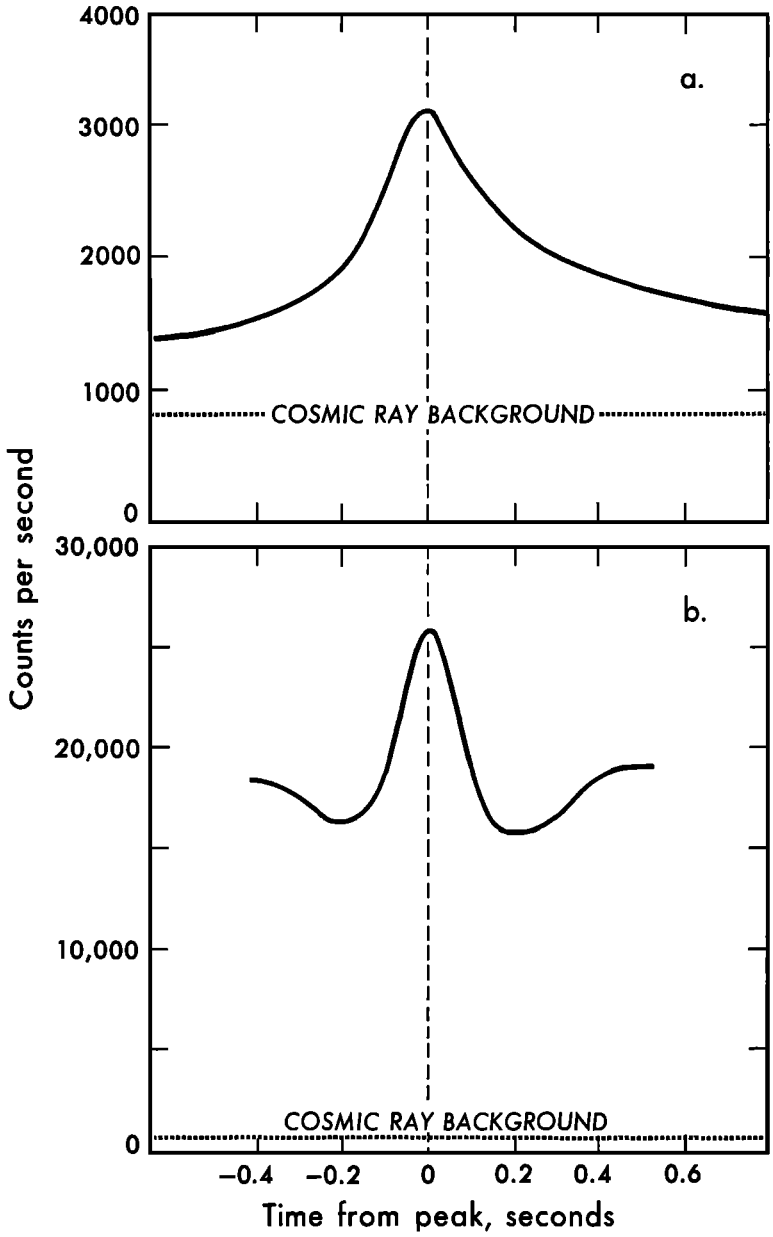

Fig. 12. Results of the autocorrelation of many individual microburst shapes. (*a*) The result from flight 341 on August 30, 1963. (*b*) The result from flight 346 on September 20, 1963.

time for the composite of August 30, 1963, is appreciably longer than the other. We also note a large difference in the X-ray flux associated with the microbursts encountered in the two flights.

The two composites shown in Figure 12 were each constructed from subcomposites, four in one case and five in the other. These consisted of a part of the total number of microbursts analyzed. Figure 13 shows the set of subcomposites before final averaging and linearizing. This technique of dividing the data into several

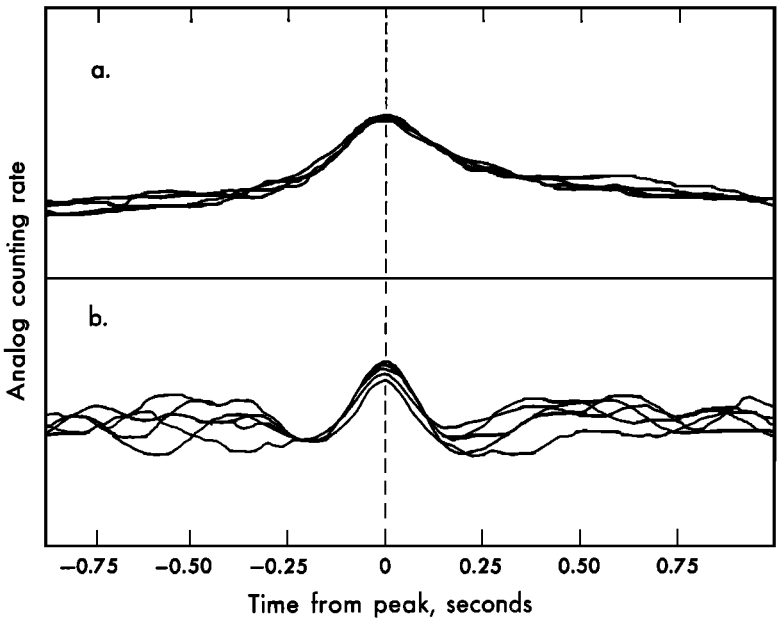

Fig. 13. Modified Chree analysis on microburst trains encountered on (*a*) flight 341 and (*b*) flight 346. Absence of side peaks shows that no near-periodic behavior is present in the microburst spacing.

sections is a direct means of arriving at a measure of statistical significance. As can be seen from Figure 13, the variation at the main peak between the subcomposites is small, showing that the standard deviation of points on the final composites must be small. A visual inspection of many individual microbursts also bears out the conclusion that the statistical averages closely represent the properties of single microbursts.

The variance of microburst shapes from the composite has also been studied. The counting rates employed in the analysis were true counting rates obtained from the analog counting rate by use of the in-flight calibration sequence. To remove rapid statistical fluctuations, the analog rate was averaged over 10-msec intervals by use of electrical filters before the strip chart graphing. The true counting rate can be found from such a presentation to an accuracy of about 20%. The true rates at fixed time intervals from the peak were next determined. These times were ± 0.1, ± 0.2, and ± 0.3 sec. The difference between the peak rate and the counting rate at one of these points, for example -0.2 sec, divided by the time interval 0.2 sec then gives the average slope of the counting rate increase. The corresponding slope over the interval 0 to $+0.2$ is then determined. The ratio of this rate of rise to the rate of fall is then a measure of the asymmetry of the microburst about its peak. A slope ratio of unity is a symmetrical microburst.

About 150 representative microbursts encountered on August 30, 1963, were analyzed in this way. On this occasion the microbursts were well separated from each other and emerged clearly from the background. The ratio of the slopes from first appearance above background can therefore be reliably determined. The results of these studies are shown in Table 1. Included there are the rise to fall ratios for the composite obtained from the same flight. The rise to fall ratios are seen to correspond fairly well, confirming the result that the microbursts of August 30, 1963, have shorter rise than fall times except near the peak where they tend to be symmetrical. Far from the peak these microbursts become highly asymmetrical owing to the long time it takes for the counting rate to decay to the cosmic ray background. The standard deviations given in the table are obtained directly from the data. They are quite large, reflecting the fact that, though micro-

TABLE 1. Microburst Symmetry Ratios

	Time Interval from Peak			
	±0.1 sec	±0.2 sec	±0.3 sec	To Background Level
From 150 individual microbursts	1.14 ± 0.7	1.43 ± 0.6	1.33 ± 0.4	2.8 ± 1.6
From composite of 150 microbursts	1.21	1.30	1.27	

bursts all tend to have much the same profile, rather large variations occur.

Peak X-ray flux of microbursts. A visual inspection of strip chart graphs shows that the peak X-ray intensity varies greatly from one microburst to another. Furthermore, the composite microbursts shown in Figure 12 obtained on separate balloon flights differ in peak counting rate by at least a factor of 8. A study was made of 460 microbursts from the August 30, 1963, flight to obtain further information on this point. The true counting rate in the 30- to 60-kev window was obtained from the analog rate as previously described. The frequency distribution of peak counting rates was then found. This distribution had its highest values at low peak counting rate and fell off rapidly toward higher rates. More than half the peak rates were less than 1600 sec^{-1} above background. One per cent of the peak rates were over 4800 sec^{-1}, and only 1 out of the 460 microbursts exceeded 15,000 sec^{-1}. The X-ray flux between 30- and 60-kev energy can be obtained roughly from the above numbers by dividing by 76 cm^2. The microbursts on September 20, 1963, emerged from an intense and variable auroral zone X-ray background. Study of the peak counting rate frequency distribution was less accurate because of this background, but some remarks can be made. The peak rates above auroral zone and cosmic ray backgrounds were much higher than for the August 30, 1963, flight. Peak counting rates of 15,000 sec^{-1} above backgrounds were common. The distribution of peak counting rates again fell off rapidly with increasing rate. Few microbursts had counting rates greater than 40,000 sec^{-1}.

X-ray energy spectrum. It is possible to study in a limited way the photon energy spectrum during a microburst with the two channels of LCRM data which were continuously available. As discussed above the mean photon energies in the two channels are 40 and 80 kev. Although the photon energy spectrum is incompletely specified by the two channels, they do provide a reliable, consistent indication of energy spectrum changes. The counting rate ratios at various times within a microburst were determined from simultaneous strip chart graphs of the analog counting rates in the two energy channels. The procedure for recovering the true counting rate in both channels was identical to that used for the time profile study. After subtracting the backgrounds, the ratio of high energy counting rate to low energy counting rate was calculated at nine different times during the microburst. The ratio could be determined in this way with an accuracy of better than 30% for the 10-msec sample.

On September 20, 1963, the microbursts rose from an intense, variable auroral zone X-ray background. The counting rate ratio for the X-ray background was 0.3 ± 0.1, so that the background at these times consisted predominantly of low energy photons. Study of the high to low energy counting rate ratio for sample microbursts showed that the ratio was constant during the entire microburst. The photon spectrum thus did not change during these microbursts. The ratio was 0.5, showing that the photons composing the microbursts were somewhat harder than the accompanying background. The high to low energy counting rate ratio was constant also for the September 29, 1963, microbursts.

A detailed study was made of the counting rate ratios at the nine times during a microburst for 150 individuals from the August 30, 1963, flight. The averages of the 150 determinations for each of nine times during the microbursts are shown in Figure 14. This ratio as a function of time during the microburst shows

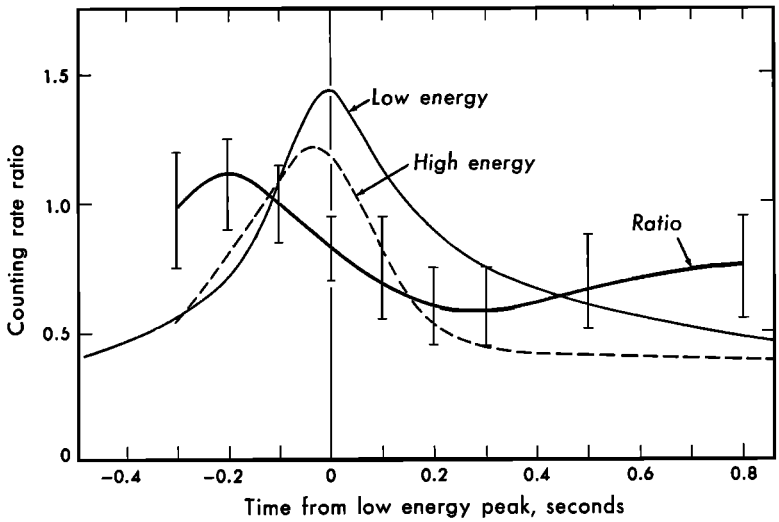

Fig. 14. Result of the analysis of X-ray energy information for August 30, 1963, microbursts. It is seen that high energy photons peak about 30 msec ahead of the low energy photons.

that at early times the photons are harder than at later times. Although the error bars are large, the smoothness of the curve connecting the data points favors the validity of this interpretation. Also plotted in Figure 14 are the composite microburst already shown and a high energy profile derived from the low energy composite one by multiplying by the counting rate ratio. Note the large counting rate ratio indicating harder X rays while the composite microburst is rising and the smaller counting rate ratio meaning softer X rays while the composite microburst is decaying. This has two interesting consequences. First, the peak of the derived high energy microburst is displaced about 30 msec ahead of the low energy peak. This has been confirmed by direct observation on the relative times of the two peaks from the strip chart graphed analog counting rates. Second, the long decay of the low energy microburst discussed in detail in the time profile study is wholly of lower energy X rays. This result is directly confirmed by study of individual microbursts in both the high and low energy channels on strip chart graphs. The microbursts as seen in the high energy channel are nearly symmetrical, whereas in the low energy channel they have a distinctly slow decay relative to their rise.

Spacing and periodic studies of microbursts. Examination of the analog counting rate graphed on strip charts for the September 20, 1963, set revealed a marked tendency for the microbursts to occur in trains of typically five microbursts, the time between microbursts being typically about 0.5 sec. Often these intervals appeared to be regular at about the full microburst width, giving the whole train the appearance of several sine wave cycles. Figures 9*b* and 10 show some of these trains. The highly variable spacings between these trains were typically 10 sec. In some of the trains the counting rate in the spaces between the microbursts would decrease to the X-ray background as in Figure 9*b*; in others it would remain high, thereby giving a webbed appearance as in the trains of Figure 8*c*. This effect often became quite pronounced, so that the trains were better described as slow increases of the same length as a microburst train with small microbursts superposed on it. Single and closely spaced pairs of microbursts occurred infrequently. The August 30, 1963, set had an entirely different appearance. Often the microbursts appeared singly as in Figures 9*a* and *c*, with typically 10-sec spacings between them. When microbursts occurred in trains they had an irregular appearance. The September 29, 1962, set had features common to both the August 30 and September 20, 1963, microburst events. In that case there were many trains

containing only three microbursts, and isolated single microbursts were numerous.

A power spectrum analysis according to the methods of *Blackman and Tukey* [1959] was carried out on the September 20, 1963, microburst trains to determine any periodicities. To concentrate the analysis on those microbursts occurring within trains and thereby increase the effective data to noise ratio, only sections of data which contained microburst trains were digitized. These sections of digitized analog counting rate containing a total of about 1200 microbursts were placed end to end to eliminate the uneventful data between them. Since periodicities were being determined over time intervals short compared to the length of the data sections, this artificial deletion of uneventful data did not create errors. The digital sampling time interval and the maximum lag were chosen to place periodicities of several tenths of a second near the center of the observable power spectrum. This particular power spectrum analysis would reveal periods between 0.1 and 3.0 sec. The power spectrum analysis and the data system were checked with two sets of test data. First, a 0.2-sec period sine wave was mixed with noise of much larger amplitude which obscured it from visual detection. The spectral estimate of these data showed a strong peak at 0.2 sec, however, showing the great sensitivity of the power spectrum analysis to small amplitudes of a definite period. Second, for check and comparison purposes, analog counting rate data were obtained from radioactive source signals passed through a flight quality unit kept in the laboratory for such purposes. The output was digitized in the same way as the X-ray data and was power spectrum analyzed. As would be expected, the spectral estimate shows no significant peaks. This result is shown in Figure 15*b*.

The digitized microburst data were divided arbitrarily into ten equal sections, and each was power spectrum analyzed separately. A point by point average and standard deviation was then taken of the ten spectral estimates. This technique of dividing the whole length of data into separately analyzed sections provides a di-

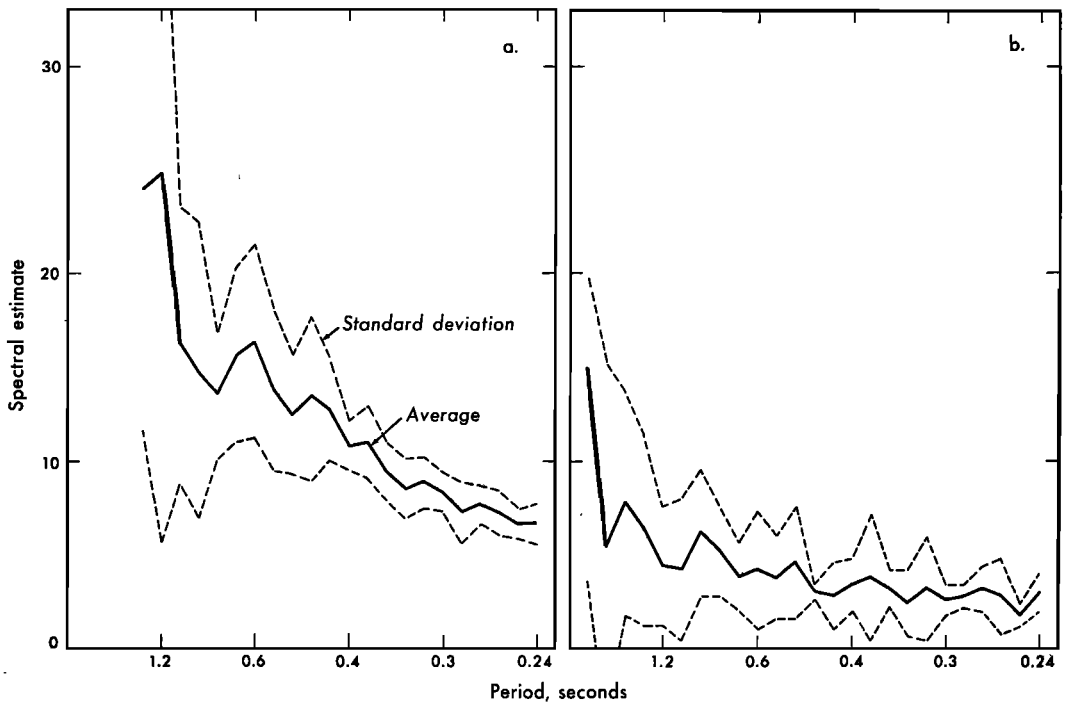

Fig 15. (*a*) Power spectrum analysis of microburst spacings within train events. (*b*) An analysis carried out in an identical way on radioactive source data shown for comparison. The power spectrum of the auroral zone X-ray data shows a barely significant peak at 0.6 sec.

rect means of evaluating the statistical significance of the results. The final average spectral estimate and the standard deviation of the variations among the ten sections are shown in Figure 15*a*. The peak at 0.6 sec is considered to be just barely significant by comparison with the standard deviation and the other peaks. This peak is remarkably weak when we consider the large and frequent counting rate variations within the trains. Since the power spectrum analysis is sensitive only to clearly defined periodicities, this indicates that the trains of microbursts, contrary to visual appearances, are not strictly periodic. The spectral estimate increase at long periods is due to the slow variations in the X-ray background.

The power spectrum studies have shown that periodicities are not a prominent feature of these microburst data. To uncover time patterns in the microburst trains that are not strictly periodic but that may be nonetheless significant for interpretation of this phenomenon, a modified Chree analysis has been applied to some of the data. Such an analysis can be expected to find a near-periodic pattern such as a slowly changing period, or a jittering period. To do this the analog counting rates in microburst trains containing five or more individuals were digitized, and the peak of a large microburst near the center of the train was marked. The trains were then superposed with the marked peaks coinciding. This analysis was used on several separate sections of data to provide estimates of statistical significance. It was found that all sections were in essential agreement. The results of the analysis on sixty microburst trains from August 30, 1963, are shown in Figure 13*a*. It is seen that side peaks are now absent. The results of the analysis on sixty microburst trains from September 20, 1963, are shown in Figure 13*b*. There is close agreement among the sections only for the central microburst. The side peaks do not occur, despite the fact that the trains contain many large microbursts on both sides of the reference peak.

Both the power spectrum analysis and the modified Chree analysis have failed to reveal any regular pattern in the temporal relations between individual microbursts. Faced with this situation, we have investigated the possibility that the microbursts occur in a purely random way. The method was to study the distribution of spacings in time between adjacent microbursts. The occurrence of random events is described by the Poisson probability distribution:

$$p(r, t) = \frac{(At)^r e^{-At}}{r!}$$

where p is the probability of r events in time interval t, and A is the average number of events per unit time. Now the distribution of spacings between random events is the same as the probability distribution of time intervals with no events in them. Setting r equal to zero gives the spacing distribution e^{-At}. The mean spacing for this distribution is at $t = 1/A$. For events of a finite width in time such as microbursts, spacings smaller than a certain minimum cannot be obtained. Therefore the spacing distribution for microbursts if they occur randomly will be the exponentially decaying one with a drop-off to zero at small spacings. Any significant departures from this will indicate that microbursts are not occurring randomly.

All microbursts greater than a minimum size that occurred during a forty-five–minute period on August 30, 1963, were selected visually from the analog counting rate graphed onto strip charts. This stretch of data is characterized by the appearance of many isolated microbursts and few microburst trains. The time spacings between 330 selected individual microbursts were measured and plotted against the frequency of occurrence of each spacing. Figure 16*a* shows the results of this analysis. The long tail approximates the Poisson distribution and corresponds to the spacing between the isolated microbursts. The sharp increase at small spacings which departs radically from the Poisson distribution is due to the greater number of smaller spacings within the microburst trains mentioned earlier. This shows that the microburst trains are not chance accumulations of microbursts. Spacings less than 2.0 sec were infrequent, so that the features in the distribution at times less than 2 sec are not significant.

Fifteen minutes of data from the September 20, 1963, flight were digitized, and a computer program was used to select microbursts above a certain size, then to plot the spacings. The result of this automatic analysis for 1200 microbursts is shown on an expanded time scale in Figure 16*b*. The long Poisson tail is again evi-

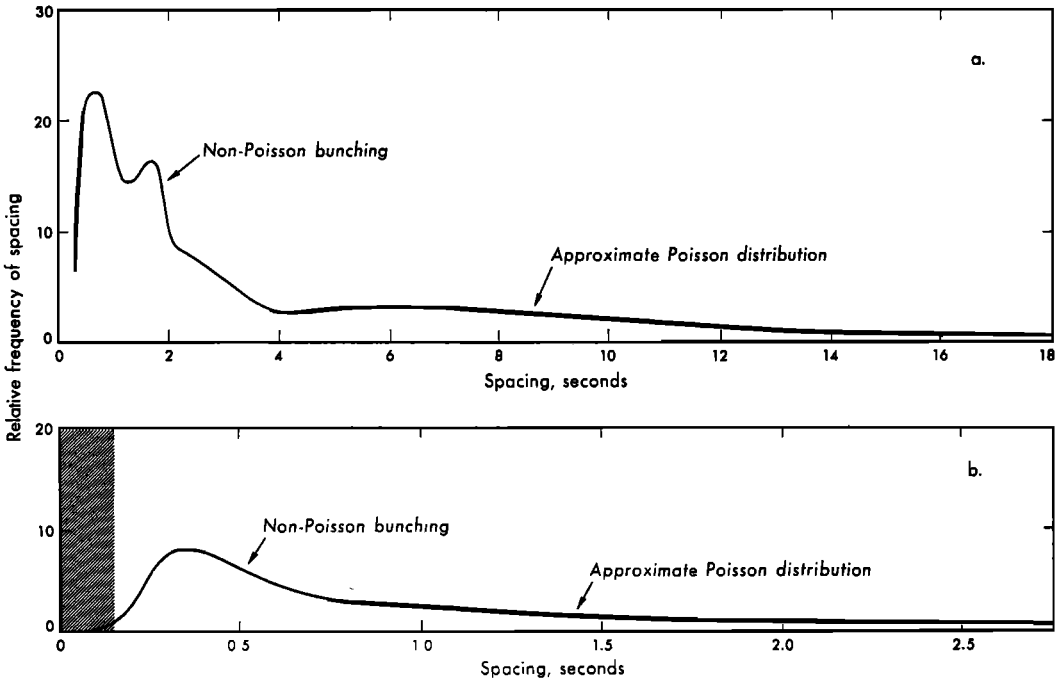

Fig. 16. Microburst spacing versus frequency of each spacing. (*a*) The microbursts analyzed were mainly isolated, single microbursts. (*b*) These microbursts were characterized by a strong tendency to occur in trains. The departure from a Poisson distribution shows the microbursts are not occurring in a purely random way.

dent and corresponds to the spacings between ends of microburst trains. Microburst trains were much more common than isolated microbursts in this particular set of data. The departure from the Poisson distribution at spacings below about one second corresponds to the numerous closely spaced microbursts within the trains. The fact that the distribution does not peak in a small range of spacings helps explain why the power spectrum and modified Chree analyses produced mostly negative results. The fall-off of this distribution at small spacings is not wholly due to an inability to resolve closely spaced microbursts, but represents also a paucity of spacings less than about 0.25 sec.

Discussion

We begin the discussion by briefly summarizing the detailed studies on microbursts described in the section on Results. We have first of all found a characteristic structure involved in the auroral zone precipitation. Microbursts are identifiable by their homogeneity in duration, in rise time, and to a lesser extent, decay time. Of the order of 5000 microbursts have appeared on our records from three separate balloon flights in different years. We believe these structures to be a common and characteristic feature of the $L = 6$ region, but their frequent presence can be revealed only by very large X-ray detectors and flexible, high information rate electronic circuitry.

The information obtained in these experiments on the energy spectrum of the X rays in microbursts shows an energy dispersion with higher energy photons arriving first at the detector and disappearing before the lower energy photons do. There is a time displacement of about thirty milliseconds between the peaks of the high and low energy photon envelopes of the same microburst. We interpret this as a velocity dispersion of the parent electrons. We infer that part of the trapped electron supply is thrown suddenly into the loss cone a considerable distance out on the line of force. When the electrons arrive at the atmosphere, the higher energy electrons lead those of low energy. We have investigated the observed 30-

msec dispersion from this point of view and find it quantitatively reasonable with respect to the bremsstrahlung response of the counter and a travel distance of the order of several earth radii. Power spectrum analysis has revealed no strong periodicities in the microburst patterns, although a barely significant peak appeared at 0.6 sec for microbursts in trains. This type of analysis is extremely demanding, since it thoroughly rejects any pattern not strictly periodic. It may therefore be of somewhat limited usefulness for these complex geophysical phenomena. The less stringent Chree analysis, however, shows no near-periodic behavior, but comparison with a random distribution of spacings does show the microburst patterns are not purely random. One must therefore attach some significance to the times between microbursts beyond their simply being related to the mean frequency of occurrence of random events. A possible significance of these spacings is discussed below.

Figures 9 and 10 illustrate the differences between microburst trains. Sometimes they are very deeply notched, returning to background between individual peaks. Other trains are webbed to varying degrees. We find, in fact, a more or less continuous gradation from the deeply notched variety through webbed ones to some that are quite smooth.

It appears that several balloon observations of microbursts have been made in the past but not recognized as such because of inadequate time resolution. The 1959 measurement shown in Figure 1 seems to be an example, with each spike possibly being an unresolved microburst train. The events reported by *Anger et al.* [1963] may be of this type, again with individual microbursts unresolved.

It is also possible that microburst events have been encountered in satellite measurements. Figure 18 in *O'Brien's* [1964] paper shows three distinct precipitating electron peaks. It is probably not possible to determine the duration and intervals between peaks in real time owing to the satellite motion, but these events reported by O'Brien seem consistent with a microburst interpretation. The electron intensity is sufficiently high so that large X-ray effects would be produced at balloon altitude.

Though we believe that the distribution of spacings between microburst trains is random, the mean spacing, the one parameter characterizing a random distribution, ought to be of some significance. The mean spacing of the trains is about 10 sec. We next remark that the supply of parent electrons can be maintained from the static supply of trapped radiation on lines of force above the auroral zone for the observed duration of the microburst phenomena, about one hour in each of the cases studied here. A possible interpretation for the microburst train phenomenon is that a disturbance existing in the outer magnetosphere untraps electrons and that their bremsstrahlung in the atmosphere produces the observed effects in our detectors. The individual disturbances must be random with a mean spacing of 10 seconds. Their duration should be a few seconds to conform to the duration of a microburst train. We note further that the magnetic pulses in the transition region discussed by *Sonnet and Abrams* [1963] are of this character judging from an inspection of the several pages of examples shown in their article. These sharp pulses occurred in an interval of earth center distance from 12.3 to 14.6 earth radii on the sunlit hemisphere. The peaks have amplitudes from a few gammas up to about 100 γ. If such disturbances propagate in the transition region and reach the magnetospheric boundary, it may be possible for them to couple to the dipole field and produce disturbances on the lines of force as far in as $L = 6$, where the microburst trains are seen. These magnetic pulses are probably strongest on the daylit hemisphere, and, as we have already noted, the microbursts appear in daylight hours. This hypothesis can be explored further with more extensive measurements of fluctuation phenomena in the outer magnetosphere and by further study of the diurnal properties of the microburst trains.

We next attempt to explain two temporal features that have appeared in the analysis of microbursts as being characteristic times associated with the trapped radiation zone:

1. Consider the shaded region in Figure 17*a*. Its length is drawn to be one-third the total arc length of the $L = 6$ line of force, and it is centered on the magnetic equator. The time required to empty out electrons of 100 kev into the atmosphere from that shaded region when one end arrives at the atmosphere is 0.2 sec.

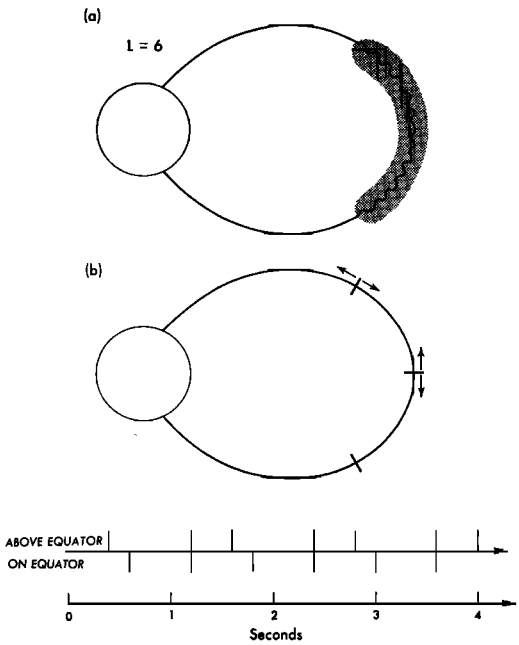

Fig. 17. A model that interprets some of the microburst time constants in terms of trapped particle motions. The center third of the $L = 6$ line of force is relatively weak and exposed to disturbances originating outside the magnetosphere. Part *a* shows this part of the line by an irregular curve. Electrons of 100-kev energy in this shaded region having appropriate pitch angle require 0.2 sec to empty into the atmosphere once this tube reaches the atmosphere. This time is close to that of the microburst width. If a fraction of the electrons in a tube precipitate at each mirroring for several successive mirrorings, electrons will appear in the atmosphere in a definite pattern corresponding to the location of the tube's center at the initial instant. This pattern is shown for the same hemisphere for two different center points. The combined pattern gives spacings of 0, 0.2, 0.4, and 0.6 sec. These spacings are typical of observed microburst spacings.

This is just the characteristic width of the microburst. For the detectors used here, their response can be shown from bremsstrahlung theory applied to this problem to be due mainly to 100-kev electrons. We also remark that the center third of the auroral zone line of force is weak and exposed to disturbances when on the sunlit hemisphere. Such disturbances may indeed be generated in the transition zone as Sonnet and Abrams' study indicates. In this view we expect particle precipitation effects to be important from this central part of the line.

2. The full bounce period for 100-kev electrons on an $L = 6$ dipole line is 1.2 sec. If the particles with small pitch angle but not in the loss cone in the shaded region of Figure 17*a* at some initial instant are followed through later times, they are seen to move away from the equator in both directions, mirror just above the atmosphere, then move across the equator into the other hemisphere. Thus if the particles initially in this region could be tagged, an observer in the northern hemisphere located at the end of this line of force would see tagged particles overhead at intervals of 0.6 sec. If another tube of tagged particles is chosen not centered at the equator but, for example, at one-third the way around a line of force, tagged particles will appear above the observer at alternating intervals of 0.4 and 0.8 sec. For other points on the line of force there will be other pairs of values always summing to the total bounce period, 1.2 sec in this example. If several points on the line of force are centers for tagged particles, an observer will see them overhead in a pattern containing many spacings less than 0.6 sec, half the bounce period in this case. As has been discussed, the spacing of microbursts when they occur in trains is concentrated in the interval 0.15 to 1 sec with a peak at about 0.4 sec. We next suppose that the rapid onset of a disturbance in the region of the $L = 6$ line centered more or less on the equator radically alters the pitch angle distribution of 100-kev electrons so that not only does the loss cone contain particles, but angles just outside the loss cone now carry large fluxes. The particles in the loss cone then move to the atmosphere and are lost. The particles just outside the loss cone move back to the equatorial region where the disturbance is still present but is now in more or less a steady state. It still, however, is postulated to have some frequency components which can reshuffle particles. Since the angles just off the loss cone have been loaded up, the smaller disturbance can fill the loss cone. These particles would then precipitate into the atmosphere about 0.6 sec after the first bunch. This process would continue until the particle supply at pitch angle near the loss cone was depleted or until the disturbance disappeared. In this way a train of electron bursts, each of duration 0.2 sec and spaced typically

0.6 sec, would appear in the atmosphere, producing the observed microburst features.

We must point out a serious difficulty in associating a simple propagating disturbance with the cause of pitch angle reshuffling discussed above. The X-ray detectors used here can see effectively over a region of sky at least 100 km in diameter. In the equatorial plane this distance transforms to about 2000 km for an auroral zone line of force. Therefore a disturbance propagating through the magnetosphere at a speed of 1000 km/sec requires about 2 sec to pass over the detector, and we should expect a rising and falling X-ray signal lasting for about 2 sec. On this view it is difficult to account for such rapid flux changes as those occurring in microbursts.

We do emphasize, however, that despite this difficulty it is possible to explain several microburst features in terms of known phenomena. The general appearance of the microburst trains resembles that of magnetic pulses in the transition zone. Further, the microbursts themselves have durations and spacings that can be understood on the basis of electron motions on the $L = 6$ line of force.

We plan to investigate further the microburst phenomenon, in particular the existence of phase differences from north to south. This may help us decide if these bursts are related to propagating disturbance in the magnetosphere.

Acknowledgment. This work was supported in part by the Office of Naval Research under contracts Nonr-222(40) and Nonr-3656(13) and its Skyhook Balloon Program.

References

Anderson, K. A., A review of balloon measurements of X rays in the auroral zone, *Univ. Calif., Berkeley, Cosmic Ray Group Preprint 64-1,* April 1964; also to be published in *Proc. January 1964 Lockheed Auroral Symp.,* Stanford University Press, Stanford, 1964.

Anderson, K. A., and D. C. Enemark, Balloon observations of X rays in the auroral zone, 2, *J. Geophys. Res., 65,* 3521–3538, 1960.

Anger, C. D., J. R. Barcus, R. R. Brown, and D. S. Evans, Auroral zone X-ray pulsations in the 1- to 15-second range, *J. Geophys. Res., 68,* 1023, 1963.

Blackman, R. B., and J. W. Tukey, *The Measurement of Power Spectra,* Dover Publications, New York, 1959.

O'Brien, B. J., High latitude geophysical studies with Injun 3, 3, *J. Geophys. Res., 69,* 13–43, 1964.

Sonnett, C. P., and I. J. Abrams, The distant geomagnetic field, 3, *J. Geophys. Res., 68,* 1233–1263, 1963.

Winckler, J. R., P. D. Bhavsar, and K. A. Anderson, A study of the precipitation of energetic electrons from the geomagnetic field during magnetic storms, *J. Geophys. Res., 67,* 3717–3736, 1962.

(Manuscript received May 18, 1964.)